Effect of antenna capacitance on the plasma characteristics of an internal linear inductively coupled plasma system

Jong Hyeuk Lim,[1] Kyong Nam Kim,[1] Jung Kyun Park,[1] and Geun Young Yeom[1,2]
[1]*Department of Materials Science and Engineering, Sungkyunkwan University, Suwon, Kyunggi-do, 440-746, South Korea*
[2]*The National Program for Tera-Level Nanodevice, Hawolgok-dong, Sungbuk-ku, Seoul, 136-791, South Korea*

(Received 4 June 2008; accepted 16 July 2008; published online 11 August 2008)

This study examined the effect of the antenna capacitance of an inductively coupled plasma (ICP) source, which was varied using an internal linear antenna, on the electrical and plasma characteristics of the ICP source. The inductive coupling at a given rf current increased with decreasing antenna capacitance. This was caused by a decrease in the inner copper diameter of the antenna made from coaxial copper/quartz tubing, which resulted in a higher plasma density and lower plasma potential. By decreasing the diameter of the copper tube from 25 to 10 mm, the plasma density of a plasma source size of $2750\times 2350\ \mathrm{mm}^2$ was increased from approximately $8\times 10^{10}/\mathrm{cm}^3$ to $1.5\times 10^{11}/\mathrm{cm}^3$ at 15 mTorr Ar and 9 kW of rf power. © *2008 American Institute of Physics*. [DOI: 10.1063/1.2967895]

I. INTRODUCTION

High density plasma sources have been investigated for the material processing of flat panel displays (FPDs) at lower temperatures and higher processing rates. In particular, among the various high density plasma sources, inductively coupled plasma (ICP) sources have attracted considerable for uniform processing on the large area substrate of FPDs due to the easier expandability of the source.[1] However, in the case of conventional external antenna-type ICP sources, the scaling up of the source for the processing of large area substrates applied to next generation FPDs shows problems due to the thick thickness of the dielectric material separating the outside antenna coil from the plasma, and the large impedance of the antenna coil, etc. Therefore, internal antenna-type ICP sources with various types of antennas, such as the loop type, serpentine type, double comb type, etc., have been investigated in an attempt to produce uniform high density plasma over an extremely large area substrate.[2–5]

In the case of internal-type ICPs, a metallic antenna line, which is generally made from copper tubing, is inserted in the vacuum chamber and separated from the plasma by a thin dielectric tubing covering outside of the antenna line. The thickness of the dielectric tubing and the distance between the antenna line and dielectric tubing not only affects the impedance of the antenna but also changes the transmission of the electromagnetic field from the antenna to the plasma. In this study, the capacitance of an internal-type ICP antenna was varied by changing the metallic antenna line diameter, and the effect of the antenna line diameter on the electrical characteristics and plasma characteristics was investigated using a large area internal antenna-type ICP source with a double-comb-type antenna.[6,7]

II. EXPERIMENT

Figure 1(a) shows a schematic diagram of the experimental setup of the double-comb-type antenna used in this study. The processing chamber has a rectangular shape, $2750\times 2350\ \mathrm{mm}^2$ in size, for applications to large area FPD processing. The substrate size was $2300\times 2000\ \mathrm{mm}^2$. As shown in Fig. 1(a), the double-comb-type antenna consisted of eight antennas with a diameter ranging from 10 to 25 mm. One side of the antenna was alternatively connected to a 10 kW 13.56 MHz rf power generator through an L-type matching network while the other side was connected directly to the ground. The antenna was made from copper tubing to allow water cooling and the outside of the antenna was coaxially covered with quartz tubing, 33 mm in diameter and 2 mm in thickness. The characteristics of the Ar plasma were examined using a Langmuir probe (Hiden Analytical Inc., ESP) installed at the center of the chamber. The electrical characteristics of the antenna were measured using an impedance probe (MKS Inc.) installed between the matching network and antenna.

III. RESULTS AND DISCUSSION

Figure 1(b) shows a schematic diagram and electrical equivalent circuit of the antenna line, quartz tubing, and plasma for the antenna for the internal-type ICP source. As shown in the equivalent circuit, the rf voltage induced on the antenna line (V_{rf}) was divided into the following according to Kirchhoff's voltage law: Space voltage between the antenna line and the quartz (V_{ad}), the voltage in the dielectric material (quartz tubing) (V_d), the sheath voltage between the dielectric material and the plasma (V_{ds}), and the sheath voltage between the plasma and the grounded chamber wall (V_p).[8] In this circuit, due to the same current flow along the closed circuit, the voltage drop at each part is related to the respective capacitance according to the following equation:

$$C_{ad}V_{ad}=C_dV_d=C_{ds}V_{ds}=C_pV_p, \tag{1}$$

where C_{ad}, C_d, C_{ds}, and C_p are the respective capacitances of each component shown in Fig. 1(b).

In general, in an ICP system, an increase in rf power to the source alters the plasma mode from capacitively coupled

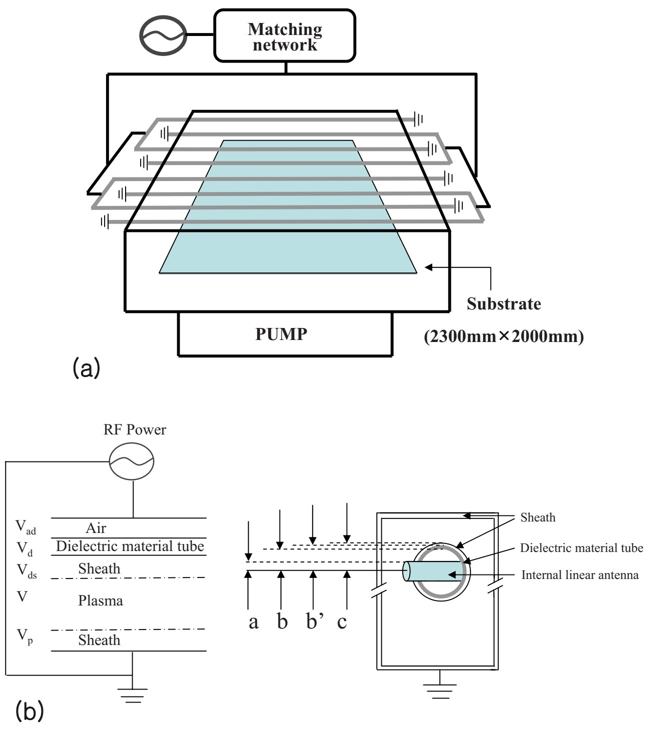

FIG. 1. (Color online) (a) Schematic diagram of a 7th generation ICP source with an internal linear antenna. (b) Schematic diagram and electrical equivalent circuit of an internal linear ICP antenna.

plasma to inductively coupled plasma mode. Due to the differences in the power absorption in the modes, there is an accompanying change in plasma characteristics, such as the plasma density, plasma potential, sheath voltage, etc. This change in the plasma mode originates from the variation in power coupling between the antenna and plasma, and the change in antenna capacitance can also affect the change in plasma mode. Therefore, the change in the sheath voltage between the dielectric tubing and plasma (V_{ds}), which originates from capacitive coupling, was estimated for different antenna diameters. The V_{ds} can be estimated by the following equation using Kirchhoff's voltage law, and Eq. (1) by assuming $V_p \approx 0$:[8,9]

$$V_{ds} = \frac{C_{ad}C_d}{C_{ad}C_d + C_{ad}C_{ds} + C_dC_{ds}} V_{\mathrm{rf}}. \tag{2}$$

The capacitance can be estimated by assuming the cylindrical geometry of the capacitor as follows:

$$C_{ad} = 2\pi\varepsilon_r\varepsilon_0/\log_{10}(b/a),$$

$$C_d = 2\pi\varepsilon_r'\varepsilon_0/\log_{10}(b'/b),$$

$$C_{ds} = 2\pi\varepsilon_0/\log_{10}(c/b'),$$

where ε_r is the relative dielectric constant (=1), ε_r' is the relative dielectric constant of quartz (=3.82), and ε_0 is the permittivity of free space ($=8.85\times10^{12}$ F/m). Using the capacitance values shown above, Eq. (2) can be changed to Eq. (3) as follows:

TABLE I. Calculated capacitance for antenna diameters of 10, 16, and 25 mm.

Diameter (mm)	C_{ad} (pF)	C_{ds} (pF)	C_d (pF)	C_{total} (pF)
10	0.11	9.2	5.1	0.106
16	0.2	7.74	5.1	0.187
25	0.7	6.3	5.1	0.56

$$V_{ds} = \frac{3.82\log_{10}(c/b')}{3.82(\log_{10}(cb/ab')) + \log_{10}(b'/b)} V_{\mathrm{rf}}, \tag{3}$$

where a, b, b', and c are the antenna radius, inside radius of the dielectric material, outside radius of the dielectric material, and the distance between the antenna center and plasma sheath edge, respectively. When the antenna diameter is changed, a is altered and c can vary according to the change in plasma characteristics. Table I shows the change in the capacitance values with changing antenna line diameter from 10 to 25 mm. The sheath distance between the outside of the dielectric material and the plasma ($d_{ds}=c\text{-}b'$) was assumed to be approximately five times the Debye length; i.e. ,$d_{ds} \approx 5\lambda_{\mathrm{D}}$, where $\lambda_{\mathrm{D}}=(\varepsilon_0 T_e/en_0)^{1/2}$.[10] As shown in Table I, the total capacitance of the antenna per unit area increased with increasing antenna line diameter from 0.106 to 0.56 pF.

Figure 2 shows the total charge (total charge$=C_{\mathrm{total}}V_{\mathrm{rf}}$) and the ratio of the sheath voltage calculated from Table I and Eq. (3). As shown in the figure, the 10 mm antenna showed the highest total charge and the total charge increased with decreasing antenna diameter due to the differences in V_{rf} induced in the antenna at the same rf power. At 9 kW rf power, the V_{rf} induced on the antenna decreased from 2.1 kV for the 10 mm diameter antenna to 0.26 kV for the 25 mm diameter antenna. However, in the case of the sheath voltage (V_{ds}) between the dielectric material and

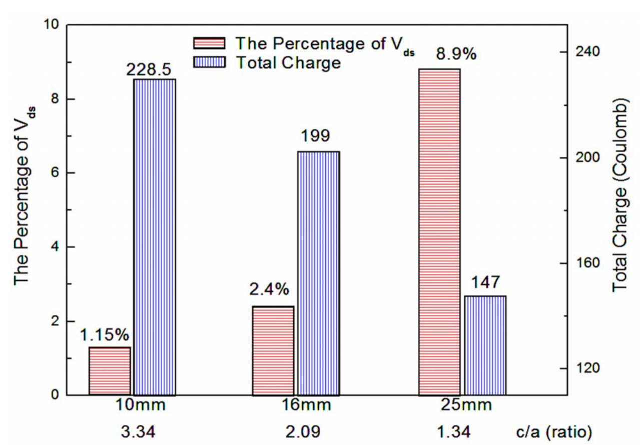

FIG. 2. (Color online) Total charge and the percentage of V_{ds} for antenna diameters of 10, 16, and 25 mm.

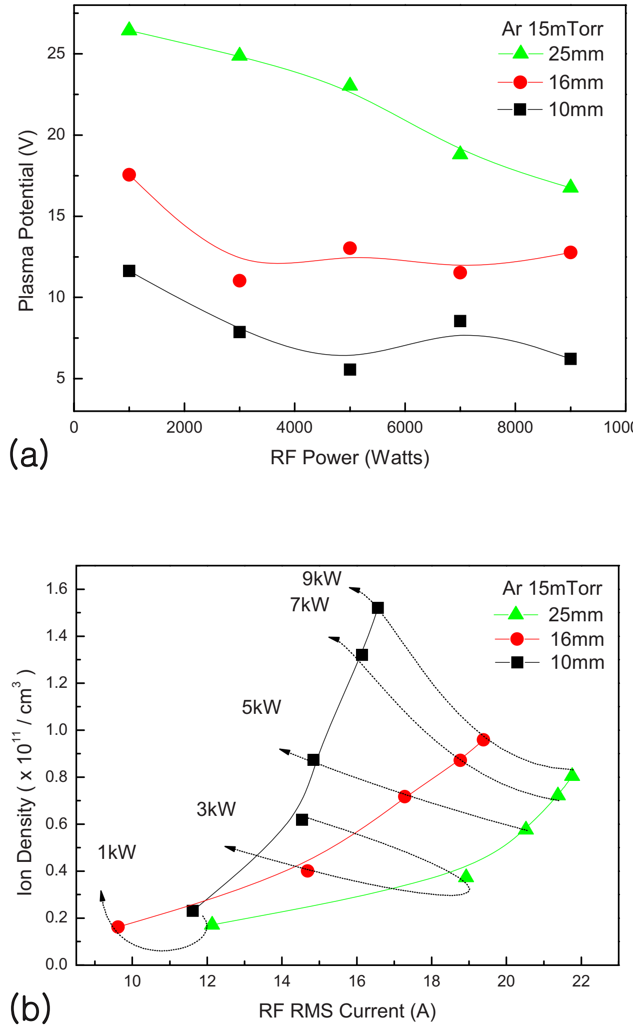

FIG. 3. (Color online) (a) Plasma potential measured as a function of the rf power for antenna diameters of 10, 16, and 25 mm. (b) Ar plasma density measured using a Langmuir probe at the center of the chamber as a function of the rf power/rf rms current at 15 mTorr Ar with antenna diameters of 10, 16, and 25 mm.

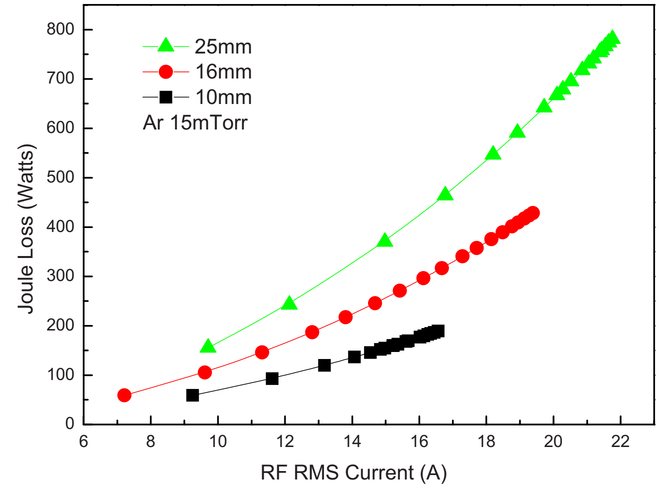

FIG. 4. (Color online) Joule loss measured as a function of the rf rms current for an antenna diameter of 10, 16, and 25 mm at 15 mTorr Ar.

plasma, due to the increase in capacitance with increasing antenna diameter, the percentage of V_{ds} to $V_{\rm rf}$ increased from 1.15% for the 10 mm antenna to 8.9% for the 25 mm antenna showing a similar V_{ds} at approximately 20–25 V.

Although V_p was assumed to be close to zero in Eq. (2), V_p can be measured. Figure 3(a) shows the plasma potential measured as a function of the rf power for different antenna diameters at 15 mTorr Ar. As shown in the figure, the increase in rf power and decrease in antenna diameter decreased the plasma potential. From the capacitance values of each component in Eq. (1), the plasma potential is related to $V_{\rm rf}$ by the following equation:

$$V_p = \frac{C_{ad}C_dC_{ds}}{C_{ad}C_dC_{ds} + C_{ds}C_pC_d + C_dC_pC_{ad} + C_pC_{ad}C_{ds}}V_{\rm rf}. \quad (4)$$

The decrease in plasma potential with increasing rf power is partially related to the increase in C_{ds} and C_p, which are approximately proportional to $\lambda_{\rm D}^{-1} = (en_0/\varepsilon_0 T_e)^{1/2}$. Therefore, an increase in rf power decreases $\lambda_{\rm D}$ by increasing the plasma density (n_0) and increasing C_{ds} and C_p. From the above equation, the decrease in C_{ad} by decreasing the antenna diameter also decreases V_p. Indeed, an increase in rf power changes the plasma mode from capacitive to inductive, and a decrease in antenna diameter decreases the percentage contribution of capacitive coupling, as shown in Fig. 2. Therefore, the decrease in plasma potential shown in Fig. 3(a) also appears to be related to the increased inductive coupling. Figure 3(b) shows the plasma density measured as a function of the rf rms current at different antenna diameters by increasing the rf power at 15 mTorr Ar. As shown in the figure, for the smaller antenna diameter, although the same rf rms current was used, a higher plasma density could be observed as a result of the increasing power transfer efficiency due to the smaller loss of rf current to the plasma.[11] At the same rf power, a higher plasma density was also obtained for the smaller antenna diameter. At 9 kW rf power and 15 mTorr Ar, a plasma density of approximately $1.52 \times 10^{11}/\mathrm{cm}^3$ could be obtained for the 10 mm diameter antenna while $8 \times 10^{10}/\mathrm{cm}^3$ was obtained for the 25 mm diameter antenna.

Figure 4 shows the Joule loss measured as a function of the rf rms current at different antenna diameters. As shown in the figure, at the same rf rms current, Joule loss was the lowest for the 10 mm diameter antenna indicating the highest rf power transfer efficiency among the antenna diameters investigated by improved the inductive coupling.

IV. CONCLUSIONS

In this study, the plasma characteristics of an internal-type ICP source were examined as a function of the antenna capacitance by varying the diameter of a copper antenna made from coaxial copper/quartz tubing. The plasma density increased from $8 \times 10^{10}/\mathrm{cm}^3$ to $1.52 \times 10^{11}/\mathrm{cm}^3$ at 9 kW of rf power and 15 mTorr Ar with decreasing antenna diameter from 25 to 10 mm. In addition, the plasma potential decreased with decreasing antenna diameter at the same rf power. The increase in plasma density and decrease in plasma potential with decreasing antenna diameter at the same rf power is related to the decreased antenna capacitance, which results in an decreased loss of rf current. Therefore, a decrease in antenna diameter resulted in an increase in inductive coupling at the same rf power by increasing the power transfer efficiency. Although the smaller antenna diameter showed more inductive coupling at the same rf power or same rf rms current in this experiment, it is believed that there is a limit to decreasing the antenna diameter that shows the highest inductive coupling.

ACKNOWLEDGMENTS

This study was supported by National Program for Tera-level Nanodevices of the Korea Ministry of Science and Technology as one of the 21st Century Frontier Programs.

[1]U. Kortshagan, N. D. Gibson, and J. E. Lawler, J. Phys. D **29**, 1224 (1996).
[2]K. Takenaka, Y. Setsuhara, K. Nishisaka, and A. Ebe, Jpn. J. Appl. Phys., Part 1 **45**, 8046 (2006).
[3]P. Colpo, T. Meziani, and F. Rossi, J. Vac. Sci. Technol. A **23**, 270 (2005).
[4]K. Eng, K. Strohmaier, R. Palmer, B. Stoner, and S. Washburn, Rev. Sci. Instrum. **68**, 2381 (1997).
[5]Y. Wu and M. A. Lieberman, Plasma Sources Sci. Technol. **9**, 210 (2000).
[6]J. H. Lim, K. N. Kim, J. K. Park, J. H. Park, and G. Y. Yeom, Jpn. J. Appl. Phys., Part 2 **46**, L1216 (2007).
[7]K. N. Kim, M. S. Kim, and G. Y. Yeom, Appl. Phys. Lett. **88**, 161503 (2006).
[8]M. A. Lieberman and A. J. Lichtenberg, *Principles of Plasma Discharges and Materials Processing* (Wiley, New York, 1994).
[9]M. Watanabe, D. M. Shaw, and G. J. Collins, J. Appl. Phys. **85**, 3428 (1999).
[10]H. Sugai, K. Nakamura, and K. Suzuki, Jpn. J. Appl. Phys., Part 1 **33**, 2189 (1994).
[11]U. Kortshagen, N. Gibson, and J. E. Lawler, J. Phys. D **29**, 1224 (1996).